EasyChair Preprint

№ 8589

Comparative Study of CFD Software for Numerical Simulation of Multiphase Flows in Secondary Metallurgy

Mario Herrera Ortega, José Ángel Ramos Banderas, Constantin Alberto Hernández Bocanegra and Alberto Beltrán Morales

August 3, 2022

Comparative Study of CFD Software for Numerical Simulation of Multiphase Flows in Secondary Metallurgy ⋆

Herrera-Ortega M. * **Ramos-Banderas J. A.** *
Hernández-Bocanegra C. A. ** **Beltrán A.** ***

* *TecNM Campus Morelia, Av. Tecnológico 1500, Morelia Michoacán, 58120 México (e-mail: mario.heortega@gmail.com, jose.rb@morelia.tecnm.mx).*
** *Cátedras-CONACyT, Av. Insurgentes Sur 1528, CDMX, 03940 México (constantin.hb@morelia.tecnm.mx)*
*** *Instituto de Investigaciones en Materiales, Unidad Morelia Universidad Nacional Autónoma de México, Morelia, Mich., 8701, 58190 México (albem@materiales.unam.mx).*

Abstract: In the present work a comparison of two softwares (comercial and open source) was made, for the numerical simulation of a multiphase flow comprising water-oil-air of a physical model of a ladle furnace used in secondary refining of steel. The results of the simulations were compared and validated with photograms of the oil aperture in the physical model. From the results, it was found that the fluid dynamic structure for both software is very simila; however, the structure of the oil aperture as well as the percentage area of exposed water differs, from one software to the other.

Keywords: CFD, water-oil-air flow, multiphase flow, OpenFOAM, Fluent.

1. INTRODUCTION

The principal aim of steel refining is to control the amount of impurities and nonmetallic inclusions, to achieve the desired chemical composition and to reach a proper temperature for the subsequent continuous casting process. Purging with an inert gas by means of porous plugs located in the bottom of the ladle creates a two phase column made up of bubbles containing kinetic energy. The accelerated bubbles generate a recirculating pattern which led to the homogenization of temperature and composition of melt, and also improves the floatation of nonmetallic particles to the top slag. However, the intensity of the momentum exchange between the two phases creates an opening in the slag layer which is detrimental to steel quality. With the growth of secondary steelmaking the interest on the mixing rate, the slag layer opening and the elucidation of the mechanism that govern the multiphase flow involved in this process, several investigations have been carried out. Some studies have focused on the influence of slag thickness (Jardón-Pérez et al., 2019) as well as the properties of slag (Amaro-Villeda et al., 2014), gas flow rate and number and location of injections of inert gas at the bottom of the ladle (Liu et al., 2011; Villela-Aguilar et al., 2020; Tan et al., 2020).

The aforementioned works reported on the literature have used commercial software to solve the equations that govern transport phenomena involved in the secondary refining process. These codes are strong technological tools and most of them are closed source software, i. e. proprietary software with the right to use, modify or share reserved to the software publisher (Liberman, 1995). Open source software as a counterpart as O'Reilly (1999) observes, is a code which is available for use, modification and redistribution without any restriction and free of charge. This type of license permit the creation of derivative works redistributed under the same terms as the original software.

OpenFOAM is license free, open source computer fluid dynamics (CFD) software (Weller et al., 1998). The works reported in literature that use OpenFOAM to solve multiphase flow present in secondary refining process are less than those reported using closed source commercial software. Kulju et al. (2015) validate a three-phase model based on a multi-fluid approach which combines the Eulerian bubble model included in OpenFOAM library and the volume of fluid (VOF) interface tracking method. They validate the results by comparing a dimensionless open-eye area with values reported in literature by Kr-

⋆ The present work has been funded by the program Becas Nacionales funded by Consejo Nacional de Ciencia y Tecnología (CONACyT).

ishnapisharody and Irons (2006). From the results the authors conclude that the multi-fluid model produces a more realistic description of the plume region and the interaction of the slag with the argon and steel phases. Liu et al. (2014) developed a numerical model which takes into account the multiphase flow and the bottom stirring in a ladle with a centered injection by means of the multiphase solver available in OpenFOAM library. The model predicts the flow in accordance with reported data by means of non-dimensional slag eye areas and transient analysis of slag eye area for different argon flow rates. Horvath et al. (2009) made a comparison of bubble column flow using two implementations of the volume of fluid (VOF) model. They found that the computational cost difference between software is not negligible and tends to favour open source software due to the lack of graphical user interface (GUI). The two formulations of the VOF model use different schemes for the solution of the discretized equations and therefore results of sharp interfaces can be different in structure.

The aim of the present work is to compare two different software, commercial and open source, with the purpose to offer an alternate solution due to differences both in use and modification of the code and to reduce license costs in future research regarding CFD simulations of industrial processes. In order to do so simulations of an air stirred physical model, comprised of water and oil to simulate the slag and steel phase are performed using both OpenFOAM and Fluent solvers. Experimental data reported in previous work (Herrera-Ortega et al., 2021) are used to validate both simulations.

2. METHODOLOGY

2.1 Physical Model Design

For the validation of the slag opening resulting from numerical simulations a 1/6 scale conical ladle made of acrylic was used. Water and mineral oil were used as working fluids to simulate the steel and slag phases respectively. The phases as well as the boundary conditions are shown in Figure 1.

The water is stirred by injecting air through a nozzle located in the mid radius of the bottom diameter of the vessel. The air flow rate in the scale model was determined by means of the Froude number (Krishnapisharody and Irons, 2013) expressed in Eq. (1).

$$\left(\frac{Q_m}{Q_p}\right)^2 = \left(\frac{\rho_g}{\rho_a}\right)\left(\frac{\rho_w}{\rho_s}\right)\left(\frac{d_m}{d_p}\right)^4\left(\frac{H_m}{H_p}\right), \qquad (1)$$

where subscripts m and p are representative of the model an the prototype, respectively, Q is the volumetric flow of the injected gas, $m^3{\cdot}min^{-1}$, d is de diameter of the nozzle, m; H, is the height of liquid, m; ρ_g, ρ_a, ρ_w, and ρ_s are the densities of argon, air, water, and steel, respectively.

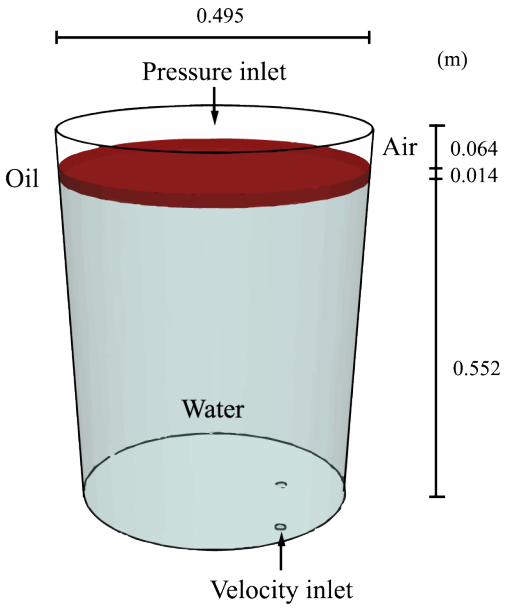

Fig. 1. Phases and boundary conditions used during the numerical simulations.

For the analysis of the slag eye area, images were taken from the top view of the physical model and extracted every second until the bath reaches a quasi-stable state. Then processed with the help of image processing software. The experimental setup is shown in Figure 2.

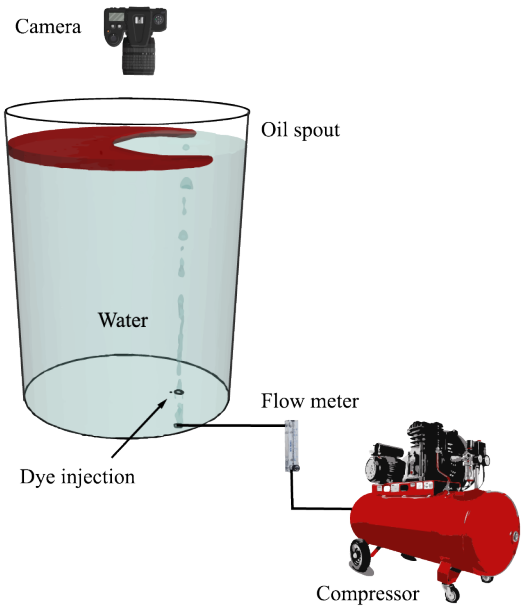

Fig. 2. Experimental setup of the physical scale model.

2.2 Numerical Model

The computational domain for the simulations was made from the dimensions of the physical model listed in Table 1.

Table 1. Dimensions of the physical model.

Parameter	Dimension, m
H_w	0.552
H_o	0.014
H_n	0.083
D_t	0.495
D_b	0.467
D_n	0.020
r/R	0.118

where H_w is the height of water, H_o is the thickness of the oil layer, H_n is the height of the nozzle entry, D_t and D_b are the top and bottom diameter of the conical vessel, respectively; D_n is the diameter of the nozzle and r/R is the location of the nozzle with respect to the bottom diameter of the vessel.

The properties of the materials used in the numerical simulations of the multiphase system are listed in Table 2.

Table 2. Properties of the materials used in the simulations.

Material	Density $kg \cdot m^{-3}$	Viscosity $kg \cdot m^{-1} \cdot s^{-1}$	Surface Tension $N \cdot m^{-1}$
Water	998.2	0.001003	-
Air	1.225	1.7894×10^{-05}	-
Oil	889	0.1589	-
Interface			
Water-Oil	**	**	0.04
Water-Air	**	**	0.072
Air-Oil	**	**	0.021

**Calculated by means of Eq. (5)

The following assumptions were considered in the present work:

- The fluids contained in the ladle behave as Newtonian.
- The flow is completely turbulent.
- Non-slip conditions for velocity occurs on all walls.
- Surface tension modelling is taken into account.
- Constant gas flow rate.
- Isothermal state in all simulations.

The discretization of the solution domain were made using two approaches depending on the software used. For the simulation run in ANSYS Fluent a structured hexaedrical mesh of 538,690 elements was used in contrast to the 789,215 element mesh generated by OpenFOAM library *snappyHexMesh* on which two levels of refinement were made in the plume zone and the slag zone. Both meshes are shown in Figure 3.

Both simulations used the volume of fluid (VOF) model on which the transport equation for the volume fraction of each phase is solved simultaneously with the continuity

a) ANSYS Meshing b) OpenFOAM

Fig. 3. Spatial discretization made with both software for comparison study.

and momentum equations. The VOF model consider two or more inmiscible fluids as one effective fluid in the whole domain on which the properties are calculated as weighted averages based on the distribution of the volume fraction. The volume fraction is defined by Eq. (2)

$$\sum_{q=1}^{n} \alpha_q = 1. \tag{2}$$

The continuity equation for the volume fraction of each one of the phases is defined by Eq. (3)

$$\frac{\partial}{\partial t}\left(\alpha_q \rho_q\right) + \nabla \cdot \left(\alpha_q \rho_q \boldsymbol{v}_q\right) = 0, \tag{3}$$

where ρ_q is the density for phase q, α_q is the volume fraction occupied by the phase q within the cell; and $\boldsymbol{q}$ is the velocity.

A single momentum equation is solved, the resulting velocity field is shared between the phases present along the numerical domain. It is shown that Eq. (4) depends on the volume fraction of all phases through the properties ρ and μ.

$$\begin{aligned} \tfrac{\partial}{\partial t}\left(\rho \boldsymbol{v}\right) + \nabla \cdot \left(\rho \boldsymbol{v}\boldsymbol{v}\right) &= -\nabla p \\ &+ \nabla \cdot \left[\mu\left(\nabla \boldsymbol{v} + \nabla \boldsymbol{v}^T\right)\right] + \rho \boldsymbol{g}\,, \end{aligned} \tag{4}$$

where ρ is the density, μ is the viscosity, ∇p is the pressure gradient, and $\boldsymbol{g}$ is the acceleration of gravity. The properties of the mixture, such as density and viscosity are calculated for the volume fraction and the properties of each phase x_q by Eq. (5)

$$x = \sum \alpha_q x_q. \tag{5}$$

To model the turbulence closure of the Navier-Stokes equations the standard $k-\varepsilon$ model with standard wall functions was used, which solves two transport equations for the turbulence kinetic energy, k; and the rate of dissipation of turbulent kinetic energy, ε, which are expressed by Eqs. (6) and (7).

$$\begin{aligned}\frac{\partial}{\partial t}(\rho k) + \nabla \cdot (\rho k \boldsymbol{v}) = \nabla \cdot \left[\left(\mu + \frac{\mu_t}{\sigma_k}\right) \nabla k\right] \\ + G_k + G_b - \varepsilon\rho,\end{aligned} \tag{6}$$

$$\begin{aligned}\frac{\partial}{\partial t}(\rho \varepsilon) + \nabla \cdot (\rho \varepsilon \boldsymbol{v}) = \nabla \cdot \left[\left(\mu + \frac{\mu_t}{\sigma_\varepsilon}\right) \nabla \varepsilon\right] \\ + C_{1\varepsilon}\frac{\varepsilon}{k}(G_k + C_{3\varepsilon}G_b) - C_{2\varepsilon}\rho\frac{\varepsilon^2}{k},\end{aligned} \tag{7}$$

here G_k, is the generation of turbulent kinetic energy due to the average of velocity gradients; G_b is the generation of turbulent kinetic energy due to the buoyancy forces; μ_t is the turbulent viscosity; $C_{1\varepsilon}, C_{2\varepsilon}$, and $C_{3\varepsilon}$ are empirical constants whose values are 1.44, 1.92, and 1.0 respectively; σ_k and $\sigma\varepsilon$ are the turbulent Prandtl number for k and ε whose values are 1.0 and 1.3, respectively.

3. RESULTS

3.1 Fluid Dynamics

The two phase zone called plume is formed due to the kinetic energy of the air bubbles injected from the bottom nozzle. Bubbles ascend and get deflected as soon as they reach the oil layer surface. This creates a recirculating pattern that goes down along the vessel walls and goes up again.

In the contours plot shown in Figure 4 velocity magnitude for both simulation can be observed, in which there is almost the same magnitude and structure for both calculations; however, the structure of the gas phase is more realistic for the calculation using OpenFOAM. This is due to the second level refinement in the plume and oil zones. Therefore the alpha fraction for the air phase shows a better resolution as it depends on the level of refinement; poor cell quality results in numerical diffusion of the air fraction calculation which can lead to unphysical results.

In Figure 5 contours lines colored by velocity magnitude are shown, in which a single dominant recirculation is observed, located in the axis of symmetry. This is due to the buoyant movement of the bubbles that are accelerating from the bottom nozzle to the top oil layer. There is a good agreement between the structures calculated by both commercial and open source software.

3.2 Slag Eye Opening

The opening of the slag layer was simulated by means of numerical simulations and physical modeling. The results of the physical modeling of the slag eye opening were

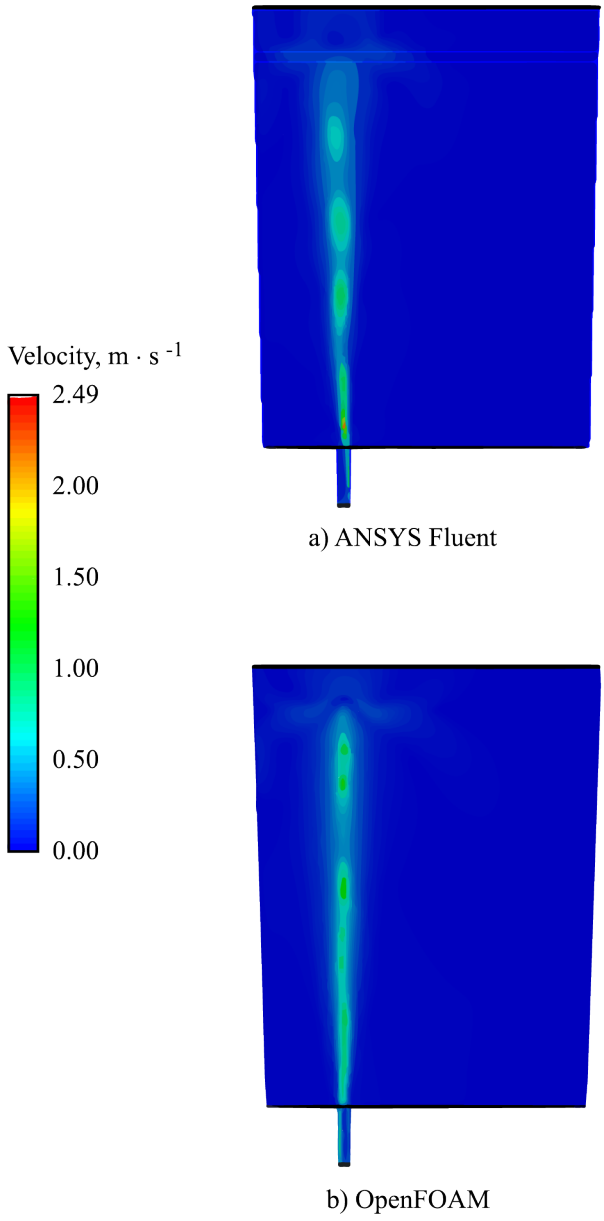

Fig. 4. Contours colored by velocity magnitude.

processed using the software ImageJ to stack several photogram into one single image and then an analysis of median of contrast to get an averaged image of the transient movement of the spout was performed. In Figure 6 the opening shape of the slag layer can be observed for both calculations and it is evident that the calculations performed with OpenFOAM have more concordance with the physical model than that with ANSYS Fluent. This can be due to the different schemes used for solving the α fraction. OpenFOAM uses an interface compression method whereas Fluent uses the Geo-Reconstruct method for sharp interfaces. There is also the fact that for the

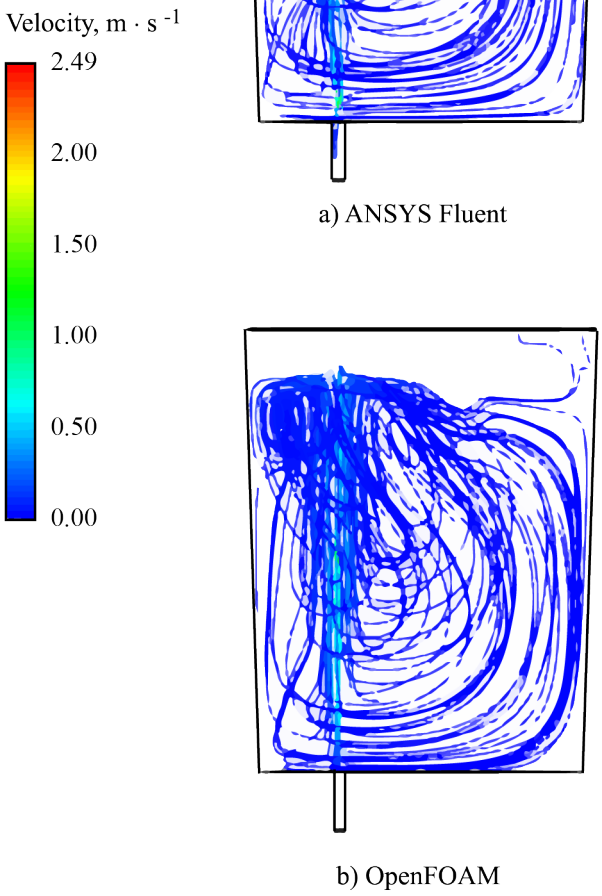

Fig. 5. Streamlines colored by velocity magnitude.

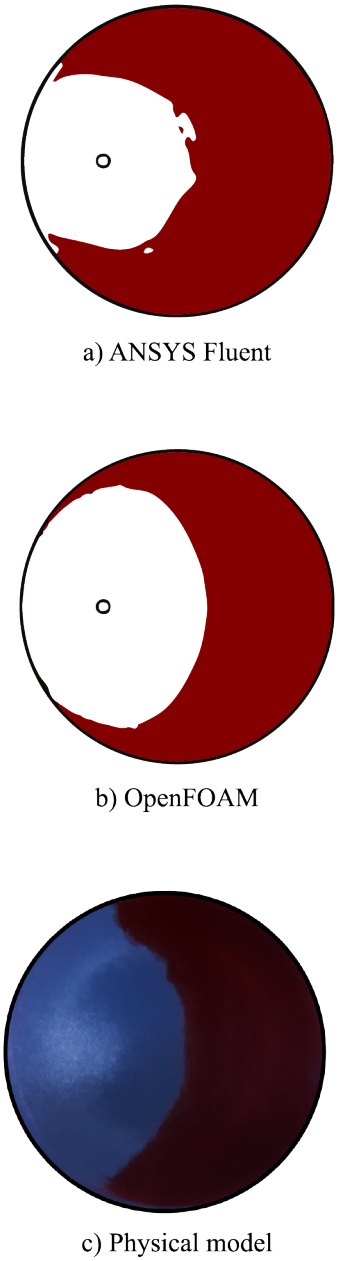

Fig. 6. Comparison of oil layer aperture from numerical simulations and physical modeling.

experimental analysis the final image is a mean representation of the flow and is hard to compare with the time-step solution from ANSYS Fluent.

4. CONCLUSION

A comparison of commercial and open source software was carried out on a multiphase numerical simulation of a physical ladle furnace model. The numerical simulation was validated by computing the slag eye opening through a physical scale model. The fluid dynamic structure is very similar for the two simulations showing the dominant recirculation however the results obtained with ANSYS Fluent has more resolution near the walls in comparison with those obtained with OpenFOAM. Slag eye opening structure is observed to be more similar to the results obtained trough OpenFOAM.

ACKNOWLEDGEMENTS

The authors want to acknowledge to the TecNM-ITM, CATEDRAS-CONACyT, IIM-UNAM Campus Morelia, CONACyT and SNI for the permanent support to the academic group of Modeling of Metallurgical Processes.

REFERENCES

Amaro-Villeda, A.M., Ramirez-Argaez, M.A., and AN, C. (2014). Effect of slag properties on mixing phenomena in gas-stirred ladles by physical modeling. *ISIJ international*, 54(1), 1–8.

Herrera-Ortega, M., Ramos-Banderas, J.Á., Hernández-Bocanegra, C.A., and Montes-Rodríguez, J.J. (2021). Effect of the location of tracer addition in a ladle on the mixing time through physical and numerical modeling. *ISIJ International*, 61(8), 2185–2192.

Horvath, A., Jordan, C., Lukasser, M., Kuttner, C., Makaruk, A., and Harasek, M. (2009). CFD simulation of bubble columns using the vof model-comparison of commercial and open source solvers with an experiment. *Chemical Engineering Transactions*, 18, 605–610.

Jardón-Pérez, L.E., González-Morales, D.R., Trápaga, G., González-Rivera, C., and Ramírez-Argáez, M.A. (2019). Effect of differentiated injection ratio, gas flow rate, and slag thickness on mixing time and open eye area in gas-stirred ladle assisted by physical modeling. *Metals*, 9(5), 555.

Krishnapisharody, K. and Irons, G. (2013). A critical review of the modified froude number in ladle metallurgy. *Metallurgical and Materials Transactions B*, 44(6), 1486–1498.

Krishnapisharody, K. and Irons, G.A. (2006). Modeling of slag eye formation over a metal bath due to gas bubbling. *Metallurgical and Materials Transactions B*, 37(5), 763–772.

Kulju, T., Ollila, S., Keiski, R.L., and Muurinen, E. (2015). Validation of three-phase cas-ob cfd-model. *IFAC-PapersOnLine*, 48(17), 1–5.

Liberman, M. (1995). Overreaching provisions in software license agreements. *Richmond Journal of Law & Technology*, 1(1), 4.

Liu, H., Qi, Z., and Xu, M. (2011). Numerical simulation of fluid flow and interfacial behavior in three-phase argon-stirred ladles with one plug and dual plugs. *Steel research international*, 82(4), 440–458.

Liu, Y.H., He, Z., and Pan, L.P. (2014). Numerical investigations on the slag eye in steel ladles. *Advances in Mechanical Engineering*, 6, 834103.

O'Reilly, T. (1999). Lessons from open-source software development. *Communications of the ACM*, 42(4), 32–37.

Tan, F., He, Z., Jin, S., Pan, L., Li, Y., and Li, B. (2020). Physical modeling evaluation on refining effects of ladle with different purging plug designs. *steel research international*, 91(6), 1900606.

Villela-Aguilar, J.d.J., Ramos-Banderas, J.Á., Hernández-Bocanegra, C.A., Urióstegui-Hernández, A., and Solorio-Díaz, G. (2020). Optimization of the mixing time using asymmetrical arrays in both gas flow and injection positions in a dual-plug ladle. *ISIJ International*, ISIJINT–2019.

Weller, H.G., Tabor, G., Jasak, H., and Fureby, C. (1998). A tensorial approach to computational continuum mechanics using object-oriented techniques. *Computers in physics*, 12(6), 620–631.

Appendix A. NOMENCLATURE

A.1 Symbol Description

$C_{1-3\varepsilon}$:	Turbulence model constants.
d_m:	physical model diameter, m.
d_p:	Full scale prototype diameter, m.
$\boldsymbol{g}$:	Gravitational acceleration, $m \cdot s^{-1}$.
G_b:	Generation of turbulence kinetic energy due to buoyancy.
G_k:	Generation of turbulence kinetic energy due to velocity gradients.
H_m:	Physical model bath height, m.
H_p:	Full scale prototype bath height, m.
k:	Turbulent kinetic energy, $J \cdot kg^{-1}$.
p:	Pressure, Pa.
Q_m:	Physical model gas flow, $Nm^3 \cdot min^{-1}$.
Q_p:	Full scale prototype gas flow, $Nm^3 \cdot min^{-1}$.
$\boldsymbol{v}$:	Velocity, $m \cdot s^{-1}$.

A.2 Greek symbols

α:	Volume fraction.
ε:	Dissipation rate of turbulent kinetic energy, $m^2 \cdot s^{-3}$.
μ:	Molecular viscosity, $Pa \cdot s$.
μ_t:	Turbulent viscosity, $Pa \cdot s$.
ρ:	Density, $kg \cdot m^{-3}$.
ρ_a:	Air Density, $kg \cdot m^{-3}$.
ρ_g:	Argon Density, $kg \cdot m^{-3}$.
ρ_s:	Steel Density, $kg \cdot m^{-3}$.
ρ_w:	Water Density, $kg \cdot m^{-3}$.
σ:	Surface tension, $N \cdot m^{-1}$.
σ_k:	Turbulent Prandtl number for k.
σ_ε:	Turbulent Prandtl number for ε.